

Influence of Tangent Pinch Points on the Energy Demand of Batch Distillations: Development of a Conceptual Model for Binary Mixtures

Karina Andrea Torres and José Espinosa*

INGAR-CONICET-UNL, Avellaneda 3657, S3002 GJC Santa Fe, Argentina

ABSTRACT: This contribution explores the influence of tangent pinch points on the performance of batch distillations of highly nonideal binary mixtures and its incorporation into a conceptual modeling framework under the assumption of a rectifier with an infinite number of stages. First of all, the $y-x$ diagram is divided into three regions taking into account both the inflection point (IP) in the phase diagram and the slope of the equilibrium curve at $x_D = 1$. After that, limiting values for the reflux ratio and distillate composition; namely, r^* and x_D^* , are calculated for the instantaneous still composition x_B with the aid of region-dependent algorithms, which incorporate the tangency condition in different ways. Finally, the instantaneous column performance is estimated taking into account the selected operation mode; i.e., constant reflux ratio or constant distillate composition. Applied to the mixture acetone–water, results for complete simulations are presented in terms of both rectification advance and operation time. A brief comparative study on the minimum energy demand required for a given separation as estimated from models with and without tangent pinches is also carried out.

1. INTRODUCTION

The influence of tangent pinch points on the minimum energy demand of a given separation has been thoroughly investigated for the case of continuous distillation of binary mixtures. The appearance of tangent pinch points in highly nonideal mixtures is related to the existence of inflection points in $y-x$ phase diagrams, which in turn are generated from inflections in the isobaric $T-x-y$ diagram.¹

When the equilibrium $y-x$ diagram has no inflections, minimum energy demand is determined as usual by using the McCabe–Thiele method. An infinite number of stages is required in each section of the column just above and below to the feed stage. A pinch with the composition of the feed (feed pinch point) controls the separation. On the other hand, the minimum reflux ratio for highly nonideal mixtures exhibiting inflections in their equilibrium $y-x$ curves is frequently characterized by one operating line just touching the isobaric equilibrium curve. The pinch location (tangent pinch point) is away from the feed stage, and only one section of the column requires an infinite number of plates as shown in Figure 1.

A more interesting approach, because it can be extended to more than two components, is the application of bifurcation theory to the estimation of the minimum reflux ratio.² By using these ideas, tangent pinch points can be represented as turning points in the diagram pinch composition versus reflux ratio. The mentioned authors extend the “zero volume” method to incorporate the influence of inflections points in phase diagrams on the minimum energy demand of a given separation. More recently, Lucia et al.³ introduced the concept of shortest separation lines which is used to find minimum energy requirements in distillation. For the case of mixtures showing tangent pinch points, they proposed a new approach that takes the general form of a nonlinear programming (NLP) problem.

Contrary to the extensive development of this subject in the field of continuous distillation, the minimum energy demand in the presence of tangent pinch points for batch distillations has deserved only little interest, perhaps as a consequence of considering that the “instantaneous performance” of a batch rectifier

can be estimated as a subcase of continuous distillation. However, as it was highlighted in a previous paper,⁴ differences between the two modes of operation can be observed when comparing the instantaneous performance of a batch rectifier and a continuous column with a feed composition equal to that of the still (see Figure 13 and Table 8 of the mentioned paper).

In batch distillation of binary mixtures, the occurrence of tangent pinch points, which in turn can be viewed as saddle-node bifurcations of reversible profiles,⁴ is checked in advance by searching for an inflection in the equilibrium curve.

The composition of the inflection point x_{IP} divides the composition simplex into two regions for the instantaneous still composition x_B . While for a still composition on the right of the inflection point (Region II), limiting values of the reflux ratio and distillate composition [r^* and x_D^*] are calculated assuming a bifurcation of the pinch profile at x_B ; a still composition on the left of x_{IP} (Region I) does not represent a bifurcation point and therefore, a tangent pinch $x_P \neq x_B$ must be found to calculate [r^* and x_D^*]. As it will be explained later, a third zone (Region 0) located near the heavy component vertex must be also considered. The right border of Region 0 is calculated from the intersection of a line through $x_D = 1$ with the slope of the equilibrium curve at $x_P = x_D$, with the equilibrium curve. Tangent pinch points do not control the separation in this region, and hence, no calculations of limiting values for the reflux and distillate composition are needed.

Once [r^* and x_D^*] are calculated, instantaneous performance calculation of the rectifier for a given reflux ratio r (operation at constant reflux) or distillate composition x_D (operation at constant distillate composition) is performed.

Beginning from an initial still composition x_{i0}^B , results from the instantaneous performance of the rectifier are used to estimate

Received: September 13, 2010

Accepted: March 29, 2011

Revised: March 9, 2011

Published: April 08, 2011

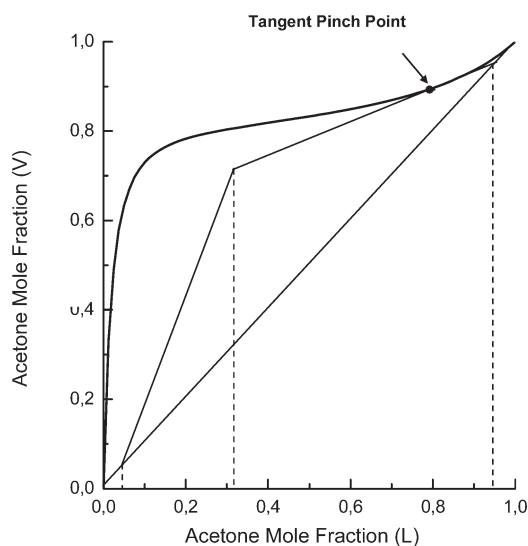


Figure 1. Phase diagram for the mixture acetone–water at 101.3 kPa and tangent pinch situation for a given feed, distillate, and bottom compositions in the case of continuous rectification.

component recoveries as functions of the rectification advance by integration of a conceptual model first introduced by Salomone et al.⁵ Time dependency of component recoveries can then easily be obtained for given values of the initial amount of feed M_0 charged in the still and either the vapor flow rate V or the operation time per batch t_p .

Finally, results of a comparative study on the minimum energy demand required for a given separation as estimated from models with and without tangent pinches are also reported.

Issues like novelty, academic relevance and practical interest of the conceptual model presented here together with related future research lines are summarized at the end of the paper.

Applied to the mixture acetone–water, this contribution is the continuation of a series of papers on the determination of minimum energy requirements of batch distillations with the aid of pinch theory-based conceptual models. The main bibliography concerning previous developments can be encountered in the works of Torres and Espinosa⁴ and Espinosa et al.⁶

2. PHYSICOCHEMICAL DATA AND INFLECTION POINT CALCULATION

In order to allow the comparison of results between the instantaneous performance of a batch rectifier and a column with 100 stages simulated in Hysys,⁷ physicochemical data for the mixture acetone–water were taken from Hysys database. While nonidealities in the liquid phase are modeled through the Wilson parameters, the extended Antoine equation is used to estimate vapor pressures.

The composition of the inflection point (IP) x_{IP} must obey the equality $(d^2y/dx^2)|_{x_{IP}} = 0$. In order to calculate x_{IP} , a method based on the improved memory method for the solution of a nonlinear equation or error function (Shacham⁸) is adopted. The method is used to solve nonlinear equations of the form $f(x) = 0$ by approximating the inverse function of $f(x)$, namely $x = \Psi(f)$, through inverse interpolation with continued fractions and evaluating the inverse function for $f = 0$. The x found value is the root of the nonlinear equation; i.e., $x^* = \Psi(0)$. The algorithm requires the evaluation of a series of points (x_0, f_0) , (x_1, f_1) , ..., (x_n, f_n) , and it

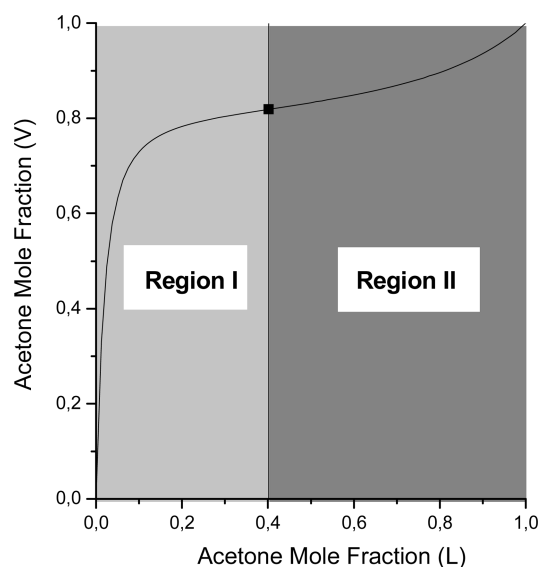


Figure 2. Inflection point mole fraction and still composition regions for the mixture acetone–water.

demands the smallest number of function evaluations in comparison with other methods as a consequence of using the information from previous iterations to generate greater order estimations of the inverse function (lineal, quadratic, etc.). Two initial points (x_0, f_0) and (x_1, f_1) must be calculated to start the algorithm in such a way that $f(x_0)f(x_1) < 0$.

To solve the problem, the mole fraction of the light component is used as iterative variable and the numerical approximation of the second derivative of the equilibrium curve with respect to the liquid mole fraction of the light species is adopted as an error function. Needed first derivative dy/dx is analytically calculated from the analytical derivatives with respect to the composition and temperature of properties like vapor pressures and activity coefficients.^{9,10} Figure 2 shows the obtained composition for the inflection point $x_{IP} = 0.4019$, which in turn determines two still composition regions with a completely different behavior in terms of minimum energy demand operation of a rectifier fed with a vapor stream in equilibrium with an instantaneous still composition x_B . The appearance of a third region near the water vertex will be explained later.

3. INSTANTANEOUS RECTIFIER PERFORMANCE AND TANGENT PINCH POINT CONDITIONS

The key of the conceptual model is the estimation of the instantaneous performance of the rectifier corresponding to an instantaneous still composition and either a given reflux ratio (operation at constant reflux ratio, variable distillate mole fraction) or a given distillate composition (operation at constant distillate composition, variable reflux ratio). Focusing our attention on the operation at constant reflux ratio, the conceptual model must predict the instantaneous distillate composition with the aid of pinch theory.

To do that, the location of the controlling pinch point must be determined in order to perform the mass balance around an envelope relating either a node pinch (Figure 3, Envelope I) or a tangent pinch (Figure 3, Envelope II) with the unknown distillate composition. Although Figure 3 shows a special case where two pinch points control the separation, the analysis of the figure enhances comprehension of the basics of the conceptual model.

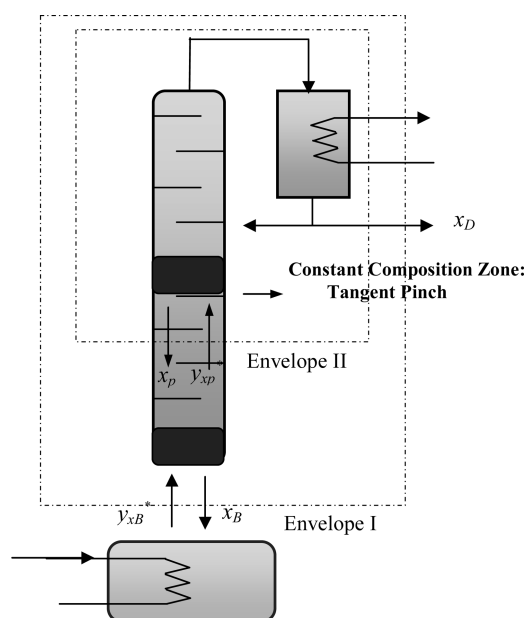


Figure 3. Schematics of an instantaneous separation with two controlling pinch points: a node pinch at the bottom and a saddle tangent pinch in the “middle” of the rectifier.

As usual, equimolal flux is assumed, and hence, the operating lines take the form of straight lines in the y – x diagram.

At pinch situation, the mass balance around either Envelope I or II becomes

$$-y_{x_p}^* + \frac{r}{r+1}x_p + \frac{x_D}{r+1} = 0 \quad (1)$$

In eq 1, $y_{x_p}^*$ is in phase equilibrium with x_p since the pinch point lies on the y – x equilibrium curve.

In case of a node pinch controlling the separation, $x_p = x_B$, and hence, eq 1 may be solved for the mole fraction of the distillate composition x_D from known values of the pinch x_p and the reflux ratio r . Otherwise, there is an additional restriction on the slope of the equilibrium curve at the tangent pinch that must be taken into account:¹

$$\left. \frac{dy}{dx} \right|_{x=x_p} = \frac{r}{r+1} \quad (2)$$

with the right-hand side of eq 2 representing the slope of the operating line of the rectifier. In this case, eqs 1 and 2 have to be solved simultaneously for the mole fraction of the distillate composition x_D and the tangent pinch composition x_p . As explained in Torres and Espinosa,⁴ the tangent pinch situation can be interpreted as a saddle-node bifurcation at x_p of the pinch profile corresponding to x_D .

4. INSTANTANEOUS RECTIFIER PERFORMANCE FOR STILL COMPOSITIONS BELONGING TO REGION II

4.1. Operation at Constant Reflux. Bearing in mind the ideas above, a method to estimate the instantaneous distillate mole fraction for a given reflux ratio r in the interval $[0, \infty]$ is outlined.

4.1.1. Calculation of Limiting Values for the Reflux Ratio and Distillate Composition. In the context of binary mixtures showing tangent pinch points, x_D^* represents the maximum feasible

Table 1. (a) Composition of the Still, its Vapor in Equilibrium, Activity Coefficient, and Vapor Pressure [kPa] of Each Component and (b) Analytical Derivatives of Activity Coefficients and Vapor Pressure at x_B

x_B	a		
	$y_{x_B}^*$	γ_i	p_i^0
0.7	0.8692	1.1394	110.3937
0.3	0.1308	2.3644	18.6808
b			
	$\partial\gamma_i/\partial x_i$	$\partial\gamma_i/\partial T$	dp_i^0/dT
	−1.4314	−0.0008	3.7044
	−0.9508	−0.0048	0.8726

composition in the distillate stream for which there exists a pinch point at the column bottom with a composition identical to that of the liquid mixture in the still; i.e., $x_p = x_B$. At this limiting situation, the pinch behaves like a tangent one, and hence, while eq 2 is solved for the limiting reflux ratio r^* , eq 1 is used to calculate x_D^* .

Table 1 gives the physicochemical data and values of the analytical derivatives needed for the solution of the equation system (1 and 2) at $x_B = 0.7$. For such an instantaneous still composition, the limiting values for the reflux ratio and the distillate composition are $r^* = 0.2954$ and $x_D^* = 0.9192$, respectively.

The analysis of the shape of the equilibrium curve in Region II (see Figure 2) allows the understanding of the calculation method. Given x_B , the tangent to the equilibrium curve at this point determines the slope of the operating line and, hence, the value of the limiting reflux ratio (eq 2). The limiting value of the distillate composition is then calculated from the intersection of the tangent with the line $y = x$ (eq 1). As $x_p = x_B$, the pinch zone is located at the column bottom just above the boiler (Figure 4).

Figure 5 shows the pinch profile corresponding to $x_D^* = 0.9192$ constructed from the McCabe–Thiele diagram for the given distillate composition.¹ While both the upper and lower stable regions represent feasible solutions of eq 1 at different values of the reflux ratio, solutions corresponding to the intermediate saddle region are physically meaningless. The solutions of the upper stable zone and the intermediate saddle region collide with each other at the composition corresponding to the mixture in the still, giving rise to a saddle-node bifurcation of the reversible profile, which characterizes the tangent pinch situation. For still compositions in Region II, the second pinch point located in the lower stable zone behaves like a nonactive pinch because the corresponding adiabatic profile starts at $x_p = x_B$ and ends at x_D^* . Note that both pinch points are located on each side of the inflection point.

4.1.2. Calculation of Instantaneous Distillate Composition x_D for $0 \leq r \leq r^*$. For values of the reflux ratio $0 \leq r < r^*$, the distillate mole fractions belong to the segment determined by the composition of the vapor in equilibrium with x_B , i.e., $y_{x_B}^*$, and the limiting distillate composition x_D^* , respectively. The instantaneous distillate composition is calculated through the lever arm rule:

$$x_D = r(y_{x_B}^* - x_B) + x_D^* \quad (3)$$

The separation is controlled by a node pinch located at the rectifier bottom as shown in Figure 4.

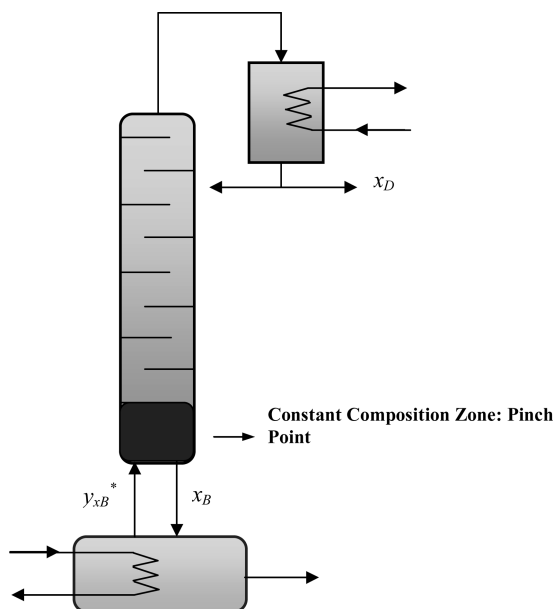


Figure 4. Schematics of an instantaneous separation controlled by a pinch of composition x_B at the bottom of the rectifier.

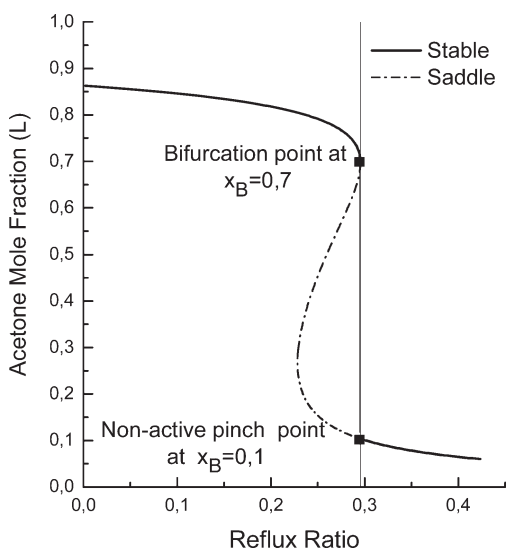


Figure 5. Reversible profile corresponding to $x_D^* = 0.9192$. The tangent pinch situation is characterized by a saddle-node bifurcation at x_B .

4.1.3. Calculation of Instantaneous Distillate Composition x_D for $r^* < r \leq r_{max}$. For values of the reflux ratio $r^* < r \leq r_{max}$, the distillate mole fractions belong to the segment determined by the limiting distillate composition x_D^* , and the light component vertex $x_D = 1$, respectively. The location of the zone of constant composition (pinch zone) in the rectifier suffers a jump from the bottom (Figure 4) to some place “in the middle” of the column (Figure 6). The controlling pinch point of unknown composition $x_p \neq x_B$ is now the tangent pinch corresponding to the bifurcation reflux ratio $r = r^{bif} > r^*$. In other words, eqs 1 and 2 are needed to describe the instantaneous performance of the rectifier.

Note, however, that the pinch behavior depicted in Figure 6, not only has a lower limit for the reflux ratio but it also presents

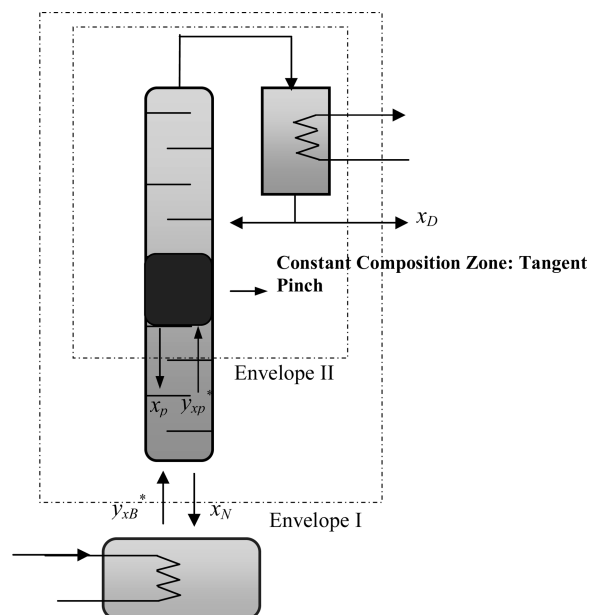


Figure 6. Schematics of an instantaneous separation controlled by a pinch of composition x_p in the middle section of the rectifier.

an upper one. In fact, the maximum value for the reflux ratio, which in turn allows a distillate of maximum purity, is obtained by applying the tangency condition at the upper bound for the still compositions in Region II:

$$\left. \frac{dy}{dx} \right|_{(1,0)} = \frac{r_{max}}{r_{max} + 1} \tag{4}$$

This limiting reflux ratio represents the maximum value for which the minimum energy demand of the column is controlled by a tangent pinch. Operation at $r > r_{max}$ is characterized by a node pinch at column top with the composition of the light component (Figure 7), and it does not represent any enhancement in product purity. At $r \rightarrow \infty$, the adiabatic profiles resemble that of total reflux. For the mixture under study, a value for $r_{max} = 5.2474$ is obtained.

In order to calculate x_p , a method based on the improved memory method for the solution of a nonlinear equation or error function⁸ is adopted. First, eq 2 is solved taking the mole fraction of the light component in the pinch x_p as an iterative variable. The error function

$$\Delta r = r^{bif} - r \tag{5}$$

is defined as the difference between the bifurcation reflux ratio r^{bif} obtained by solving eq 2 for a pinch composition x_p in the interval $[x_B, 1]$, and the operation reflux r . Once the tangent pinch composition is found, the distillate composition is computed by solving the mass balance around Envelope II (Figure 6). Finally, the composition of the liquid leaving the rectifier at the bottom x_N is obtained from the mass balance around Envelope I. Figure 8 shows the error function as a function of the tangent pinch composition.

For a given operation reflux ratio, i.e., $r = 1.5$, the algorithm provides the compositions of the pinch $x_p = 0.9408$, distillate $x_D = 0.9838$, and lower end stream $x_N = 0.7928$. Figure 9 shows the operating line obtained in the $y-x$ diagram. Table 2 summarizes the

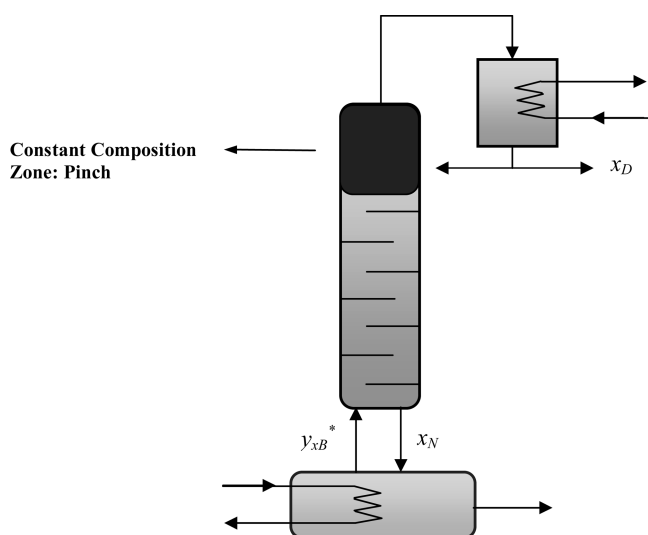


Figure 7. Schematics of an instantaneous separation controlled by a pinch of composition $x_p = 1$ in the top section of the rectifier.

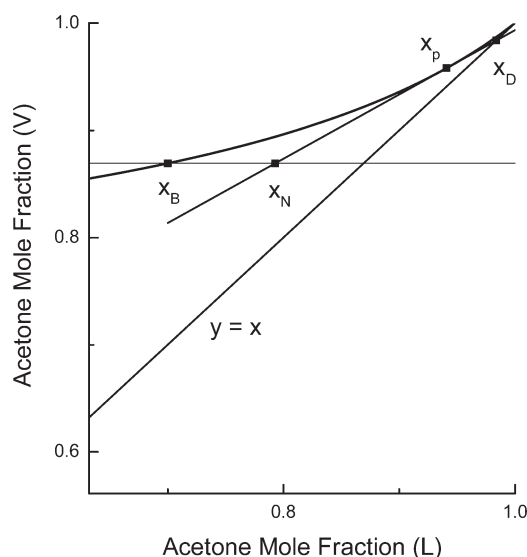


Figure 9. Operating line corresponding to $x_B = 0.7$ and reflux ratio $r = 1.5$. $x_D = 0.9838$ is calculated.

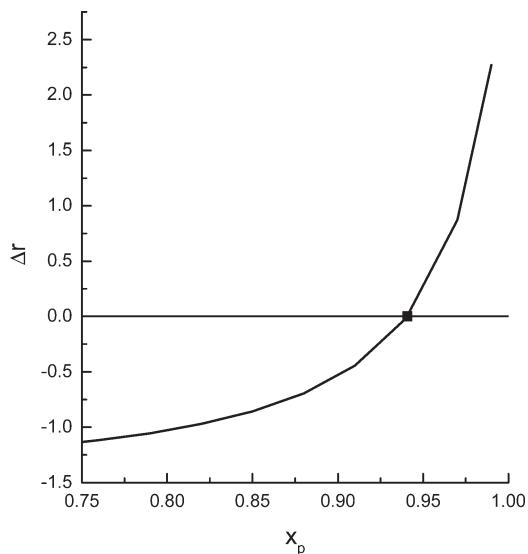


Figure 8. Error function Δr (eq 5) versus x_p corresponding to $x_B = 0.7$ and $r = 1.5$.

results of the conceptual model for the instantaneous performance of the rectifier at different reflux ratios.

In order to make a comparison between the results from the solution of the conceptual model and actual profiles of a column having 100 equilibrium stages (as an approximation to a column with an infinite number of trays), rigorous simulations with Hysys are performed for different values of the reflux ratio $r^* < r \leq r_{max}$. According to Figure 6, the feed to the rectifier is the vapor $y_{x_B}^*$ in equilibrium with the still composition x_B . To run the simulations, an arbitrary value of the vapor flow rate is set (i.e., $V = 100$ kmol/h). With these data and for a given value of the reflux ratio, the simulation provides composition and flow rates of the distillate stream (x_D, D), lower column end stream (x_N, L_N), and the corresponding values for each equilibrium stage. From the analysis of the calculated internal profile, it is possible to establish an approximate value of the tangent pinch composition as the one

Table 2. Results from the Conceptual Model for $r^* = 0.2954 \leq r \leq r_{max} = 5.2474^a$

r	x_D	x_N	x_p	Δr
0.2954	0.9192	0.7000	0.7000	
0.4	0.9341	0.7069	0.7684	-5.3060×10^{-10}
0.5	0.9444	0.7187	0.81	-1.7255×10^{-10}
0.6	0.9524	0.7306	0.8395	7.8734×10^{-9}
0.7	0.9587	0.7414	0.8617	2.4782×10^{-8}
0.8	0.9639	0.7509	0.8790	4.6121×10^{-8}
0.9	0.9682	0.7592	0.8929	6.6670×10^{-8}
1.2	0.9776	0.7789	0.9222	9.7146×10^{-8}
1.5	0.9838	0.7928	0.9408	8.2411×10^{-8}
2	0.9903	0.8086	0.9604	3.1518×10^{-8}
3	0.9967	0.8267	0.9812	5.2821×10^{-7}
4	0.9992	0.8367	0.9920	2.3469×10^{-4}
5	0.9999	0.8430	0.9987	5.7538×10^{-7}
5.2474	1.0000	0.8443	1.000	

^a $x_B = 0.7$.

corresponding to a zone of constant composition. Excellent agreement between simulations in Hysys and estimations from the conceptual model were obtained even when rigorous simulations consider the energy balance. Twelve reflux ratios were chosen for the same vapor feed. Mean and maximum relative errors in the distillate composition were adopted as a measure of the quality of the estimations. For the example considered, $\langle \epsilon_D^{rel} \rangle$ was 0.183533% while $\epsilon_D^{rel,max}$ was 0.415587%, respectively.

4.1.4. Section Summary. Figure 10 summarizes all the situations that can be found for a still composition pertaining to Region II and reflux ratios in the interval $0 < r \leq r_{max}$ in the familiar $y-x$ diagram. Figure 11 also considers the case of $r > r_{max}$.

4.2. Operation at Constant Distillate Composition. In this section, a method to estimate the instantaneous reflux ratio for a given distillate mole fraction x_D in the interval $[y_{x_B}^*, x_D = 1]$, is outlined.

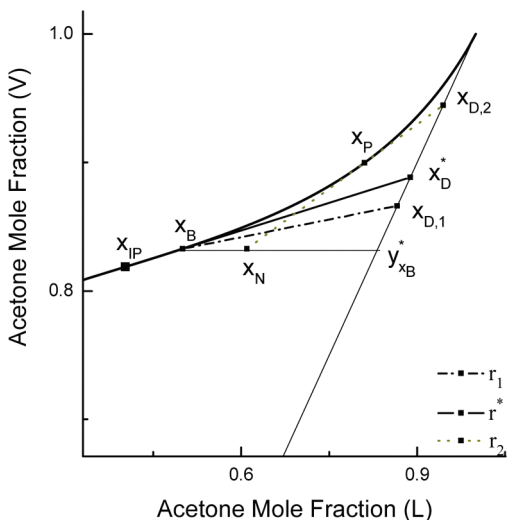


Figure 10. Operating lines corresponding to $x_B = 0.5 > x_{IP}$: $r_1 = 0.10 < r^*$; $r^* = 0.1671$; $r_2 = 0.5 > r^*$.

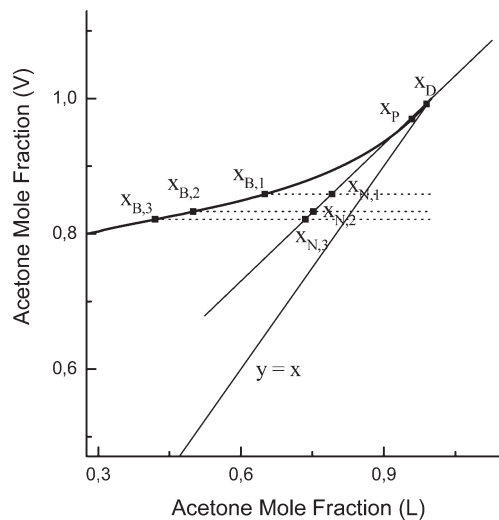


Figure 12. Operating line corresponding to $x_D = 0.99$ and to three different still compositions belonging to Region II: $x_{B,1} = 0.65$, $x_{B,2} = 0.5$, and $x_{B,3} = 0.42$.

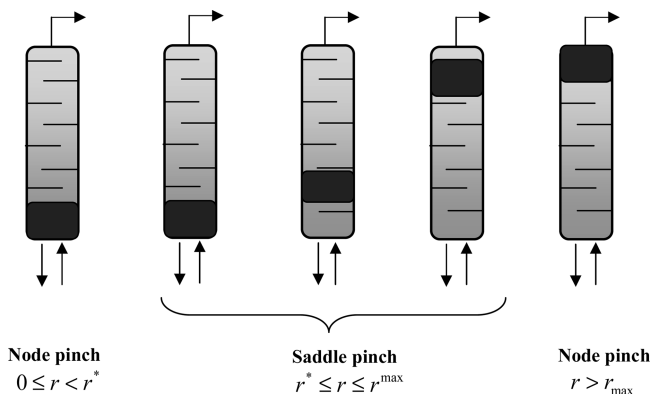


Figure 11. Operation modes of a rectifier with an infinite number of stages for a still composition belonging to Region II.

4.2.1. Calculation of Instantaneous Reflux Ratio r for $y_{x_B}^* \leq x_D < x_D^*$. As a node pinch controls the separation for selected values of the distillate mole fraction in the region $y_{x_B}^* \leq x_D < x_D^*$ (see Figures 4 and 10), the lever arm rule provides the value of the instantaneous reflux ratio:

$$r = \frac{x_D - y_{x_B}^*}{y_{x_B}^* - x_B} \quad (6)$$

4.2.2. Calculation of Instantaneous Reflux Ratio r for $x_D^* \leq x_D \leq 1$. As a tangent pinch controls the separation for selected values of the distillate mole fraction in the region $x_D^* \leq x_D \leq 1$ (see Figures 6 and 10), eqs 1 and 2 must be iteratively solved for r and x_p . Again, a method based on the improved memory method for the solution of a nonlinear equation or error function⁸ is adopted. The preprocessing step of the improved memory method is reproduced here:

Step 1. Given a distillate composition $x_D \in [x_D^*, 1]$, select $x_{p,1} = x_B$ and $x_{p,2} = 1$.

Step 2. For pinch compositions assumed in step 1, calculate r_1^{bif} and r_2^{bif} through eq 2 and the corresponding distillate

Table 3. Comparison of Results between Hysys and the IMM-Based Conceptual Model: $x_D = 0.99$

	x_B	r	x_D	x_p	x_N
hysys	0.42	1.96	0.99	0.960041	0.724324
conceptual model		1.9657		0.959357	0.735492
hysys	0.5	1.96	0.99	0.959067	0.742730
conceptual model		1.9672		0.959405	0.752898
hysys	0.65	1.96	0.99	0.958909	0.783927
conceptual model		1.9654		0.959352	0.791527

compositions $x_{D,1}$ and $x_{D,2}$ through the mass balance around Envelope II of Figure 6 (eq 1).

Step 3. Calculate the error function $\Delta x_{D,1} = x_{D,1} - x_D$ and $\Delta x_{D,2} = x_{D,2} - x_D$, defined as the difference between an estimated distillate composition and the prefixed distillate mole fraction.

Step 4. Initialize the IMM with $[x_{p,1}, x_{p,2}]$ as initial search interval for the controlling pinch composition in order to find the value of x_p (and hence, the value of r) such that $\Delta x_D \cong 0$.

Step 5. After convergence of IMM in step 4, calculate x_N through the mass balance around Envelope I of Figure 6 (eq 1).

Figure 12 and Table 3 shows the results obtained from the conceptual model for three different compositions of the liquid mixture in the still. In all the considered cases, both the composition of the tangent pinch and the value of the reflux ratio remain invariant because there is only one tangent to the equilibrium curve that points to the selected x_D .

5. INSTANTANEOUS RECTIFIER PERFORMANCE FOR STILL COMPOSITIONS BELONGING TO REGION I

5.1. Calculation of Limiting Values for the Reflux Ratio and Distillate Composition. For still compositions pertaining to Region I, x_D^* represents the composition of the distillate for which there exists two controlling pinch points: a node pinch at the column bottom with a composition identical to that of the liquid mixture in the still; i.e., $x_p = x_B$, and a tangent pinch located in the “middle” of the column as shown in Figure 3. Due to the shape of the equilibrium curve, the node pinch will lie on the left of the

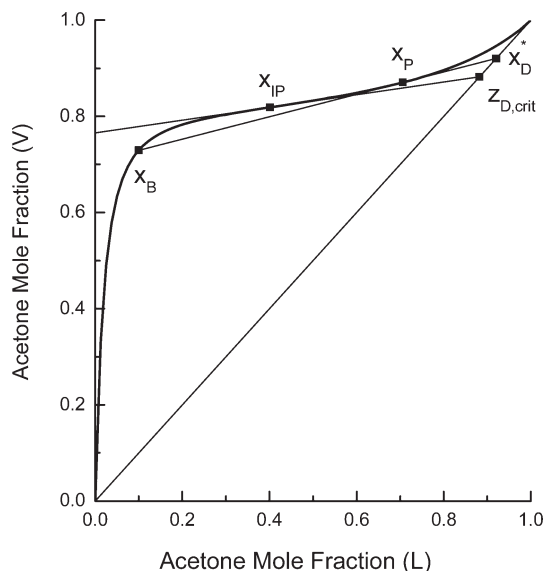


Figure 13. Limiting operating line for a still composition $x_B < x_{IP}$.

Table 4. Limiting Reflux Ratio, Distillate Composition, and Tangent Pinch Composition for Three Different Still Mole Fractions (Region I)

	$x_B = 0.1$	$x_B = 0.2$	$x_B = 0.3$
r^*	0.303469	0.197911	0.170778
x_D^*	0.920539	0.898057	0.889711
x_P	0.706729	0.577664	0.512278

inflection point and the tangent pinch on the right. Figure 13 shows an example of the limiting case.

Values for r^* and x_D^* are calculated by solving two nested IMM algorithms. The outer loop iterates over x_D while the inner loop takes x_P as the guess variable. The outer algorithm ends when x_P , x_B , and x_D are aligned.

The search for x_D^* (outer loop) is carried out in the interval $[z_{D,crit}, 1]$, where $z_{D,crit}$ is obtained from the intersection of the tangent to the equilibrium curve at x_{IP} with the line $y = x$ (Figure 13). Likewise to continuous distillation, tangent pinch points do not develop for distillate compositions below $z_{D,crit}$ and hence, this limiting value must be used to restrict the search interval. For the mixture under consideration, $z_{D,crit} = 0.882321$. The search for the tangent pinch x_P (inner loop) is carried out in the interval $[x_{IP}, x_D]$, where x_D is fixed by the outer loop.

The error function for the inner loop is given by $\Delta x_D = x_D - x_{D,calc}$, where $x_{D,calc}$ is the distillate mole fraction obtained after solving eqs 1 and 2 from a value of the search variable x_P . The error function for the outer loop is given by $\Delta m = m_{x_P} - m_{x_B, x_D}$, where m_{x_P} is the slope of the tangent to the equilibrium curve at x_P and m_{x_B, x_D} is the slope of the segment joining x_B and x_D .

Table 4 and Figure 14 show the limiting operation mode for three different still compositions belonging to Region I.

For each distillate composition in Table 4, it is possible to calculate the corresponding reversible profile. Unlike to the case depicted in Figure 5, both the tangent pinch and the node pinch are now active ones as shown in Figure 15 for $x_B = 0.1$.

5.2. Operation at Constant Reflux. In the following section, a method to estimate the instantaneous distillate mole fraction for a given reflux ratio r in the interval $[0, \infty]$ is outlined.

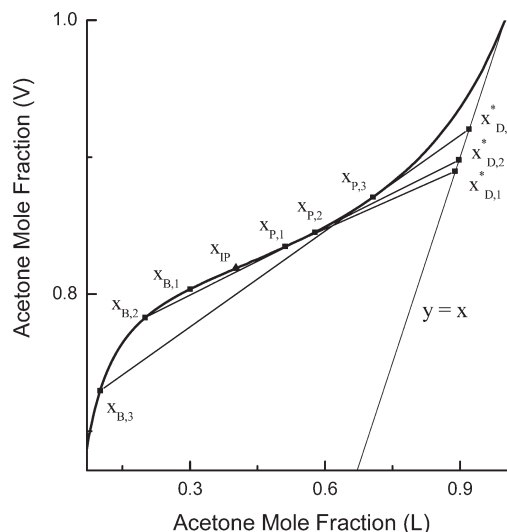


Figure 14. Still composition, tangent pinch point, and limiting distillate mole fraction for three different still compositions pertaining to Region I.

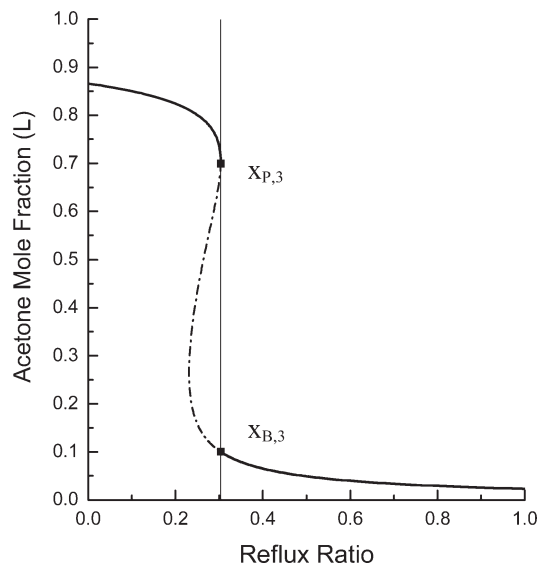


Figure 15. Reversible profile for x_D^* corresponding to $x_B = 0.1$.

5.2.1. Calculation of Instantaneous Distillate Composition x_D for $0 \leq r \leq r^*$. For values of the reflux ratio $0 \leq r < r^*$, the distillate mole fractions belong to the segment determined by the composition of the vapor in equilibrium with x_B , i.e., $y_{x_B}^*$ and the limiting distillate composition x_D^* , respectively. Then, the instantaneous distillate composition is calculated through the lever arm rule.

The separation is controlled by a node pinch located at the rectifier bottom as shown in Figure 4. For $r = r^*$, two pinch points characterize the separation as explained in the previous section.

5.2.2. Calculation of Instantaneous Distillate Composition x_D for $r^* < r \leq r_{max}$. For values of the reflux ratio $r^* < r \leq r_{max}$, the distillate mole fractions belong to the segment determined by the limiting distillate composition x_D^* , and the light component vertex $x_D = 1$, respectively. The location of the zone of constant composition of the tangent pinch suffers a jump to a new location above that of the tangent pinch corresponding to the limiting

Table 5. Comparison of Results Obtained from the Conceptual Model for $r^* < r \leq r_{max}$ and Hysys^a

	r	x_p	x_N	x_D
hysys	0.8	0.869473	0.594271	0.961415
conceptual model		0.878985	0.603481	0.963861
hysys	2	0.960153	0.705104	0.988905
conceptual model		0.960410	0.710367	0.990342
hysys	5	0.999841	0.761667	0.999841
conceptual model		0.998720	0.764435	0.999974

^a $x_B = 0.3$.

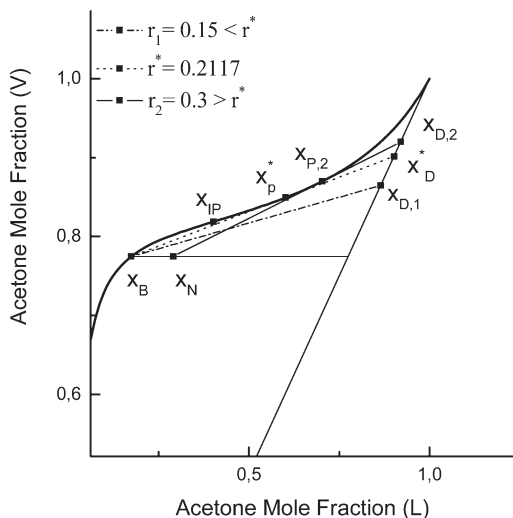


Figure 16. Three different operation modes for a still composition $x_B = 0.175$ and three different reflux ratios: $r_1 < r^*$; $r = r^*$; $r^* < r_2 < r_{max}$.

case $r = r^*$ (Figure 3). The controlling pinch point of unknown composition $x_p \neq x_B$ is now the tangent pinch corresponding to the bifurcation reflux ratio $r = r^{bif} > r^*$. In other words, eqs 1 and 2 are needed to describe the instantaneous performance of the rectifier.

As the unknown distillate mole fraction belongs to Region II, the IMM based-algorithm is the same as that explained in section 4.1.3 for still compositions pertaining to Region II. However, the search interval for the tangent pinch is restricted to the interval $[x_{IP}, 1]$ instead of $[x_B, 1]$ because no tangent pinch can develop in the interval $[x_B, x_{IP}]$ as it can be seen from the analysis of Figure 14. Table 5 presents the results obtained from the conceptual model and Hysys for three different reflux ratios above r^* and $x_B = 0.3$.

5.2.3. Section Summary. Figure 16 emphasizes the different pinch situations that can be encountered in a batch rectifier for still compositions lying in Region I. Figure 17 also includes the situation corresponding to $r > r_{max}$. In this case, the separation is characterized by a distillate of maximum purity with a node pinch located at the upper end of the column.

5.3. Operation at Constant Distillate Composition. In this section, a method to estimate the instantaneous reflux ratio for a given distillate mole fraction x_D in the interval $[y_{x_B}^*, 1]$ is briefly introduced.

5.3.1. Calculation of Instantaneous Reflux Ratio r for $y_{x_B}^* \leq x_D < x_D^*$. As a node pinch controls the separation for selected values of the distillate mole fraction in the region $y_{x_B}^* \leq x_D < x_D^*$

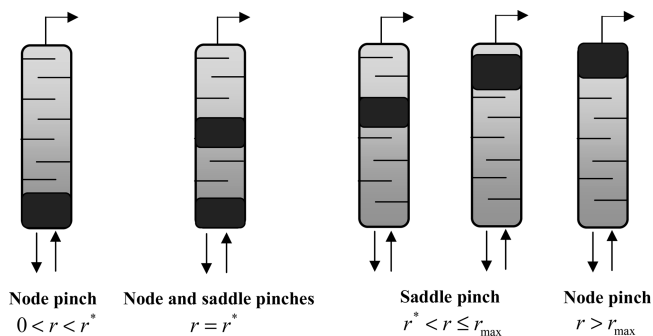


Figure 17. Operation modes of a rectifier with an infinite number of stages for a still composition belonging to Region I.

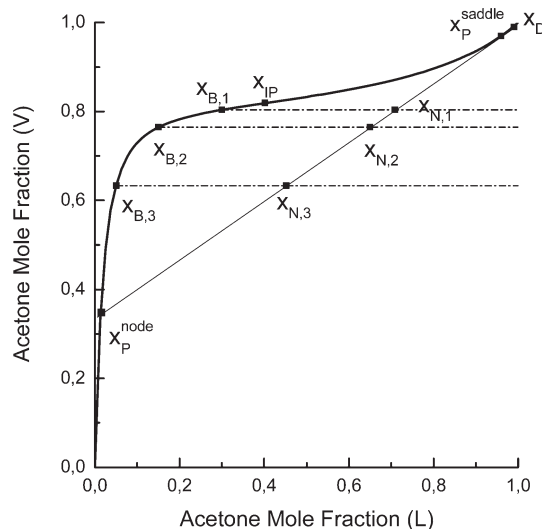


Figure 18. Operating line corresponding to $x_D = 0.99$ and to three different still compositions belonging to region I: $x_{B,1} = 0.3$, $x_{B,2} = 0.15$, and $x_{B,3} = 0.05$.

(see Figures 16 and 17), the lever arm rule provides the value of the instantaneous reflux ratio.

5.3.2. Calculation of Instantaneous Reflux Ratio r for $x_D^* \leq x_D \leq 1$. While the algorithm explained in section 5.1 must be used to obtain both r^* and x_D^* , the IMM based-algorithm developed in section 4.2.2 is appropriate for $x_D > x_D^*$. The pinch search in this case will be restricted to the interval $[x_{IP}, 1]$. Figure 18 shows the operating line corresponding to $x_D = 0.99$. Note that, for still compositions from $x_{B,1}$ to $x_{B,3}$, the separation is controlled by a tangent pinch with constant composition.

6. INSTANTANEOUS RECTIFIER PERFORMANCE FOR STILL COMPOSITIONS BELONGING TO REGION 0

By analyzing Figure 18 for $x_D = 0.99$, it is clear that this distillate purity can be achieved at the same reflux ratio from still compositions ranging from $x_B = x_B^{node}$ to $x_B = x_B^{bif} = x_B^{saddle}$ as schematically shown in Figure 3. The lower limit of the still composition $x_B = x_B^{node}$ is obtained from the intersection of the operating line formed by the points x_D and x_B^{saddle} with the equilibrium curve. In other words, the limiting operation with two controlling pinch points determines the lower limit for the composition of the still for which a distillate composition must be achieved at a constant value of the reflux ratio;

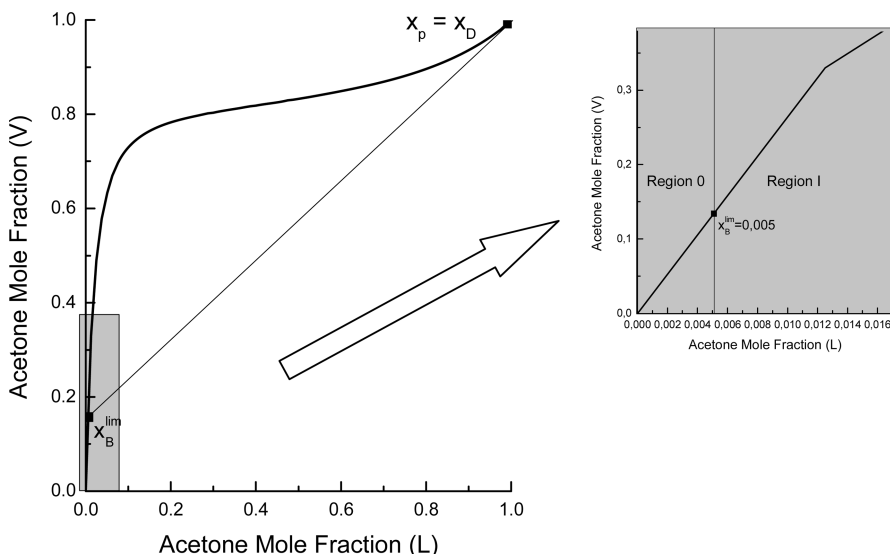


Figure 19. Graphic interpretation of the limiting still mole fraction x_B^{lim} to determine the boundaries of Region 0.

i.e., $r = r^{\text{bif}}$. For $x_B < x_B^{\text{node}}$, it will be still possible to achieve the distillate mole fraction $x_D = 0.99$ by increasing the reflux ratio above the limiting one. For these cases, separations will be controlled by node pinches located at the rectifier bottom.

The same reasoning can be made for other distillate mole fractions and in particular for $x_D = 1$. In this case, the maximum reflux ratio r_{max} obtained in section 4.1.3 can be used to calculate x_B^{lim} , defined as the minimum still composition for which a distillate of maximum purity can be achieved at column top with a node pinch at column bottom and a saddle pinch at rectifier top:

$$r_{\text{max}} = \frac{1 - y_{x_B}^{*,\text{lim}}}{y_{x_B}^{*,\text{lim}} - x_B^{\text{lim}}} = 5.2474 \quad (7)$$

By iteratively solving the equation above for x_B^{lim} in the interval $[0, x_{\text{IP}}]$, a value for the mixture acetone–water is obtained; i.e., $x_B^{\text{lim}} = 0.005$ as depicted in Figure 19. Separations for still compositions in the interval $[0, x_B^{\text{lim}}]$, which determine the locus of Region 0, are characterized by either a node pinch at the rectifier bottom for $0 \leq r \leq r_{\text{max}}^0$ or a node pinch at rectifier top for $r > r_{\text{max}}^0$, where r_{max}^0 is calculated from the lever arm rule as

$$r_{\text{max}}^0 = \frac{1 - y_{x_B}^*}{y_{x_B}^* - x_B} \quad (8)$$

As no tangent pinch can develop in this region, the lever arm rule must be used to estimate the instantaneous rectifier performance both for operation at constant reflux ratio and constant distillate composition. Figure 20 summarizes the feasible situations for a rectifier having an infinite number of trays and for still compositions in Region 0.

7. CONCEPTUAL MODEL FOR A BATCH RECTIFIER: FRACTIONAL RECOVERIES AND RECTIFICATION ADVANCE

Assuming negligible changes in tray holdups and performing mass balances around the whole batch column and the product

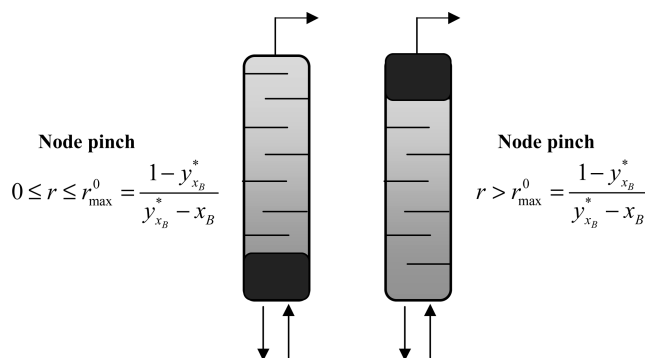


Figure 20. Operation modes of a rectifier with an infinite number of stages for a still composition belonging to Region 0.

vessel, Salomone et al.⁵ derived the following equations:

$$\frac{d\sigma_i^D}{d\eta} = \frac{x_i^D}{x_{i0}^B} \quad (9)$$

$$x_i^B = x_{i0}^B \frac{(1 - \sigma_i^D)}{(1 - \eta)} \quad (10)$$

where σ_i^D is the fractional recovery of component i in the distillate, η is the rectification advance, x_i^D is the mole fraction of component i in the distillate, and x_{i0}^B is the initial mole fraction of component i in the still. Note that η is defined as the ratio between the overall amount of product [kmol] recovered as distillate and the initial still holdup [kmol].

Equations 9 and 10 allow the modeling of the whole operation of a batch rectifier in terms of component recoveries and rectification advance instead of component mole fractions. The selected approach is very appropriate for design because specifications in batch distillation are normally given in terms of component recoveries and the vapor flow rate does not need to be specified at this level.

In order to accomplish integration of eqs 9 and 10, the algorithms presented in the preceding sections for the instantaneous performance of the rectifier must be incorporated into the

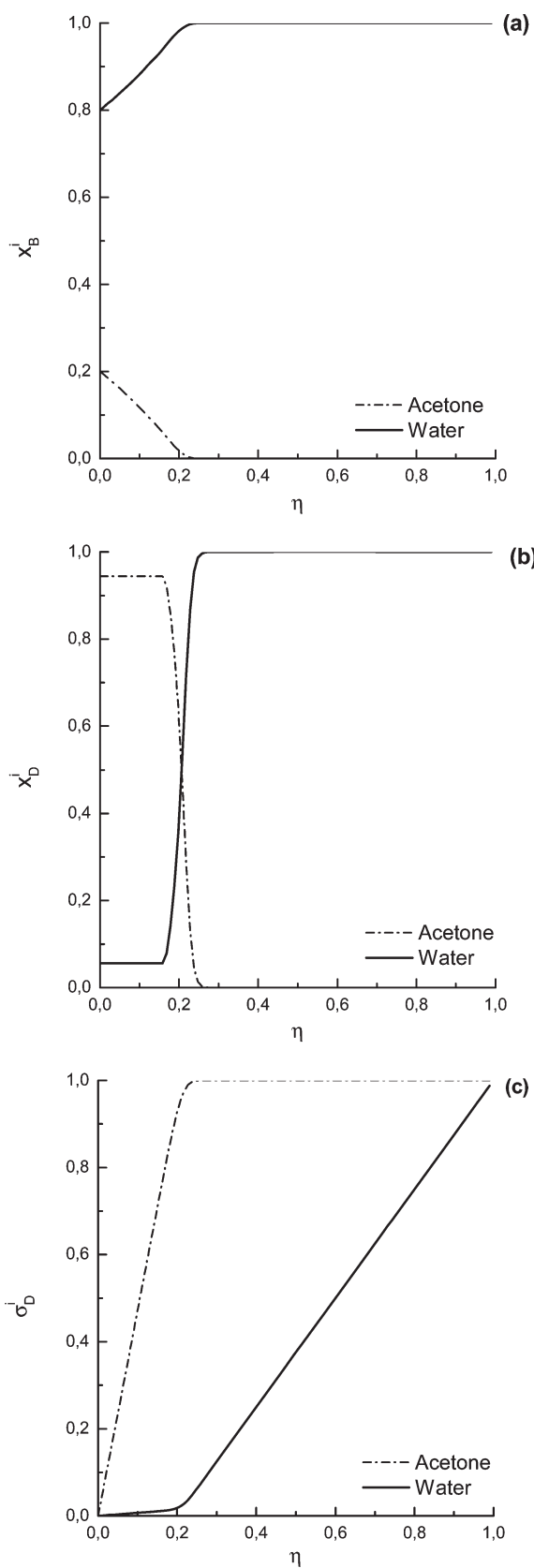


Figure 21. Evolution of (a) still compositions, (b) distillate compositions, and (c) fractional recoveries. $x_{i0}^B = 0.2$ (Region I), $r = 0.5$, and $\eta = 0.99$.

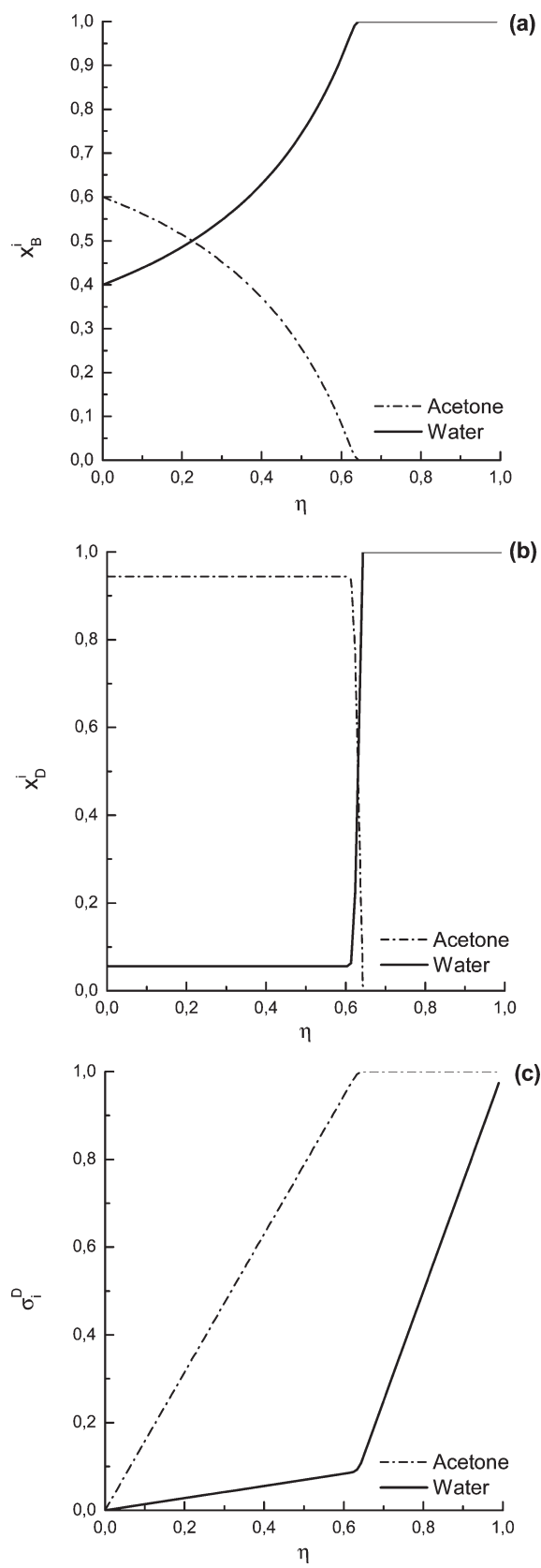


Figure 22. Evolution of (a) still compositions, (b) distillate compositions, and (c) fractional recoveries. $x_{i0}^B = 0.6$ (Region II), $r = 0.5$ and $\eta = 0.99$.

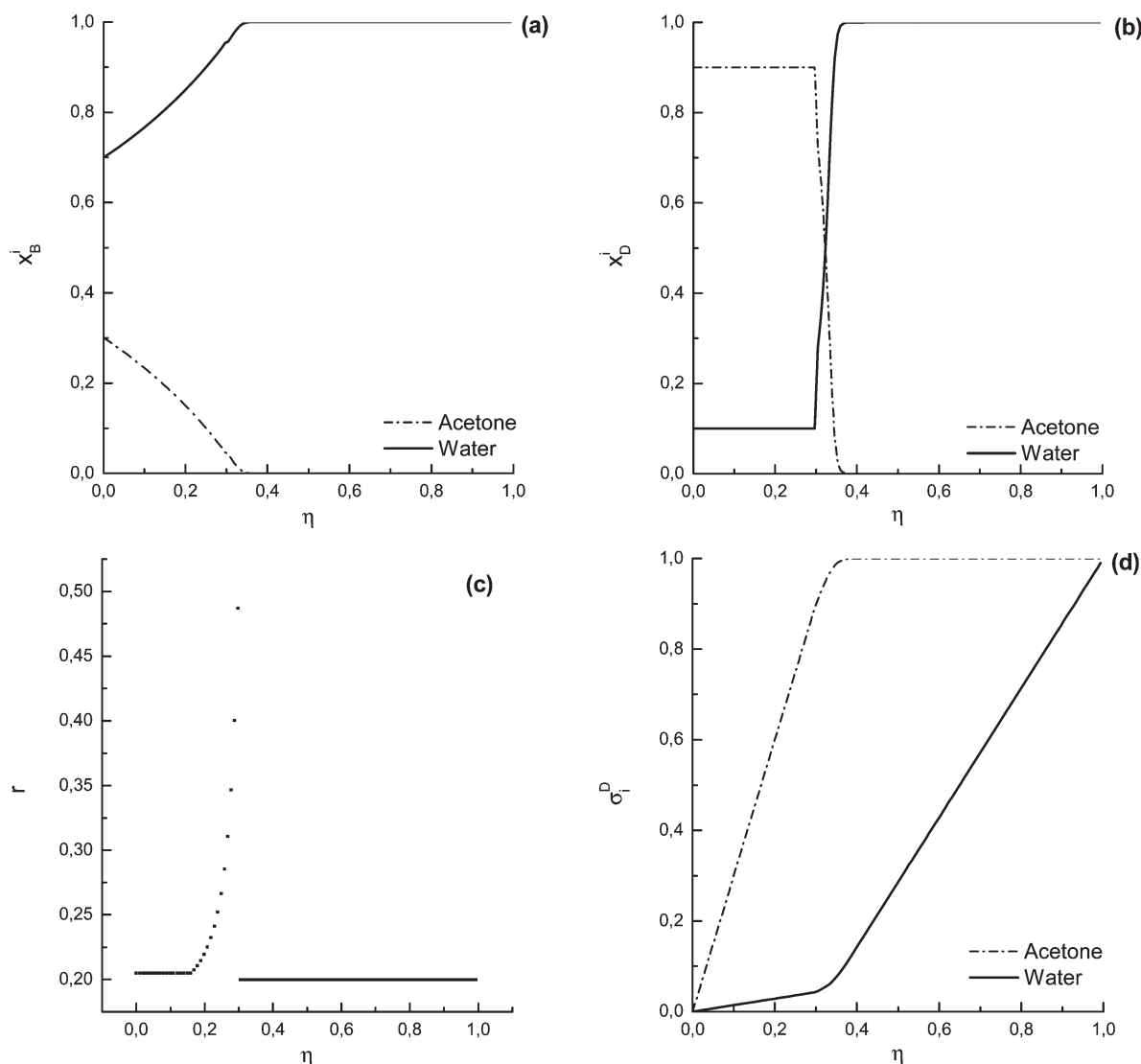


Figure 23. Evolution of (a) still compositions, (b) distillate compositions, (c) reflux ratio, and (d) fractional recoveries. $x_{i0}^B = 0.3$ (Region I), $x_D = 0.9$ during the first cut, and $\eta = 0.99$.

model. Once a new value for the instantaneous still composition is calculated from eq 10, either the instantaneous distillate composition (operation at constant reflux ratio) or the instantaneous reflux ratio (operation at constant distillate composition) needs to be estimated from the conceptual model of the rectifier. Then, eq 9 can be integrated for a differential value of the rectification advance.

7.1. Operation at Constant Reflux Ratio. Figures 21a and b and 22a and b show two typical ways of visualizing the evolution of the batch operation: still and distillate compositions versus the rectification advance. The simulations were performed for initial still compositions x_{i0}^B belonging to Region I and Region II, respectively. Both main and intermediate cuts are shown. Figures 21c and 22c depict the relationship between the fractional recovery of each component and the rectification advance. A final rectification advance $\eta \approx 1$ was selected but any desired value can be picked out.

In Figure 21b, the distillate composition remains constant $x_i^D = 0.94443$ for values of the rectification advance $0 \leq \eta \leq 0.1584$. This behavior can be explained because the bifurcating reflux ratios r^* , which depend on the instantaneous still

composition x_i^B , are lower than the operation reflux ratio $r = 0.5$; hence, the separation is controlled by a tangent pinch of constant composition which points to the same distillate mole fraction. For values of the rectification advance $\eta > 0.1584$, the bifurcating reflux ratios r^* are greater than the operation reflux, and hence, the separation is controlled by node pinch points with composition x_i^B . The lever arm rule determines the instantaneous distillate composition. Figure 16 can help the reader to understand the results.

A similar behavior is found in Figure 22b. A tangent pinch controls the separation for values of the rectification advance in the interval $0 \leq \eta \leq 0.6080$. Node pinch points with composition x_i^B control the separation for $\eta \geq 0.6080$.

It is noteworthy that for values $x_B < x_B^{\text{lim}} = 0.005$ the algorithm does not calculate any limiting value for the bifurcation reflux r^* . It estimates the instantaneous distillate composition from the lever arm rule.

7.2. Operation at Constant Distillate Composition. Figures 23 and 24 exhibit the evolution of the operation for two different initial still compositions x_{i0}^B . In both selected examples, operation at

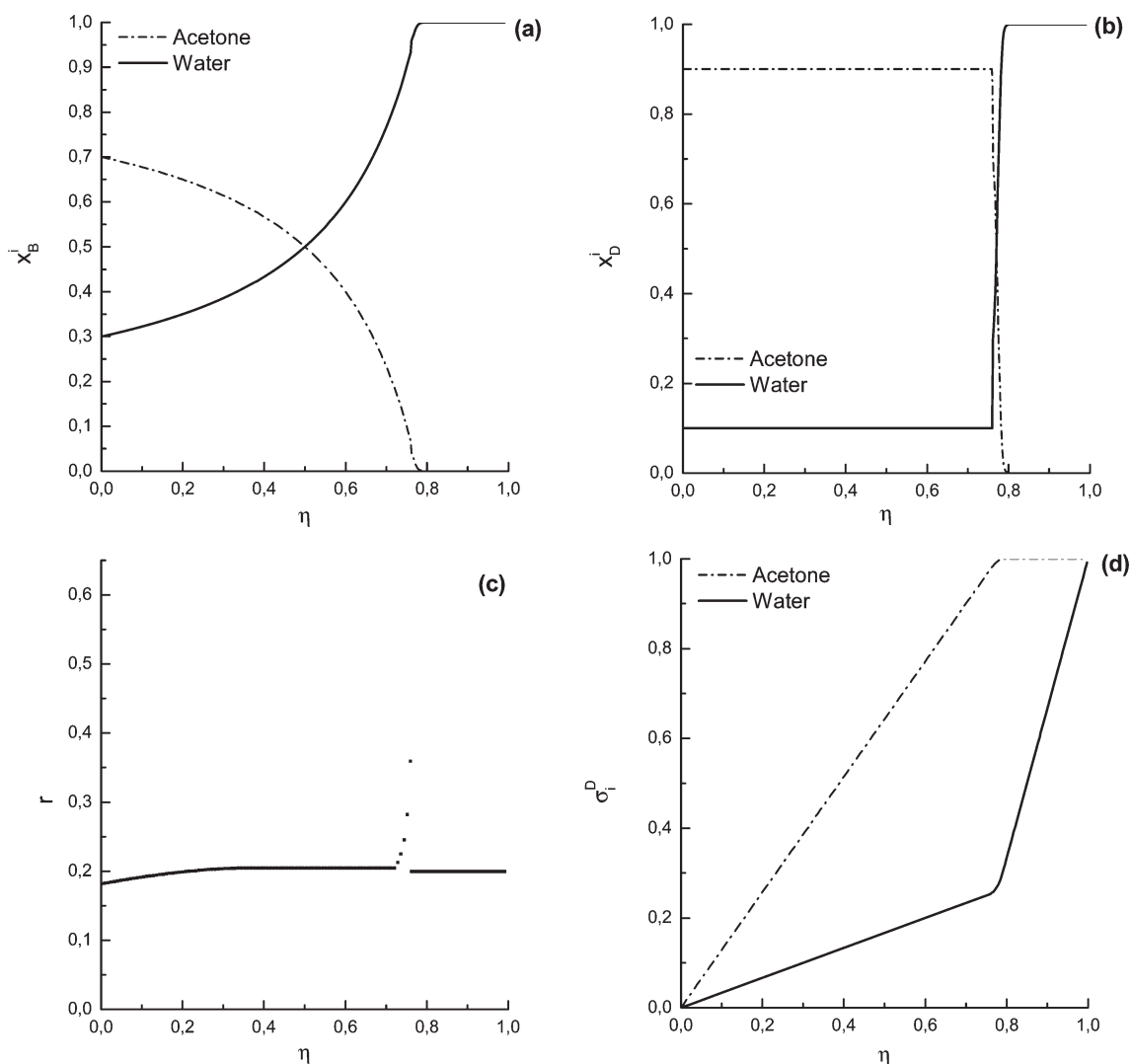


Figure 24. Evolution of (a) still compositions, (b) distillate compositions, (c) reflux ratio, and (d) fractional recoveries. $x_{i0}^B = 0.7$ (Region II), $x_D = 0.9$ during the first cut, and $\eta = 0.99$.

constant distillate composition is carried out until achieving a still content with small amounts of the light species (approximately 6% of acetone for $x_{A,0}^B = 0.7$ and 4% for $x_{A,0}^B = 0.3$). Operation at constant reflux ratio is then implemented until operation end. The change in the reflux policy from variable to constant can be clearly seen in Figures 23c and 24c.

7.3. Time Evolution of the Operation Variables. As it was explained by Bernot et al.,¹¹ a conceptual model for the whole column that decouples the variation of compositions from variation of flows and batch size can be used to estimate batch sizes, operating times, equipment sizes, utility loads, and costs for the batch distillation. To this end, the authors used in their model a dimensionless “warped” time instead of time. In this contribution, we select the rectification advance as a measure of operation progress (see eqs 9 and 10).

Products specifications for both the main and the intermediate cut can be done in terms of both purity and fractional recovery. In each case, the conceptual model can be used to estimate either the reflux ratio (constant reflux policy) or the evolution of reflux ratios (constant distillate policy) together with the corresponding rectification advance needed to meet the design specifications. To evaluate

the batch size and costs of a specific design, the operating time per batch t_p must be specified as follows:

By defining the number of batches n_b in terms of the time available t_w , the operating time per batch t_p , and the dead time t_d by

$$n_b = \frac{t_w}{t_p + t_d} \quad (11)$$

The molar amount of fresh feed per batch is then

$$M_0 = \frac{F}{n_b} \quad (12)$$

where F is the total molar amount of fresh feed to be processed in time t_w .

For selected values of F , t_w , and t_d , only one degree of freedom remains; i.e., the operating time per batch t_p . As suggested by Bernot et al.,¹¹ this variable can be eventually chosen as an optimization variable. By selecting a value for t_p , eqs 11 and 12 can be solved for n_b and M_0 .

From the results obtained at the conceptual model level, and based on the mass balance around the condenser, the vapor flow

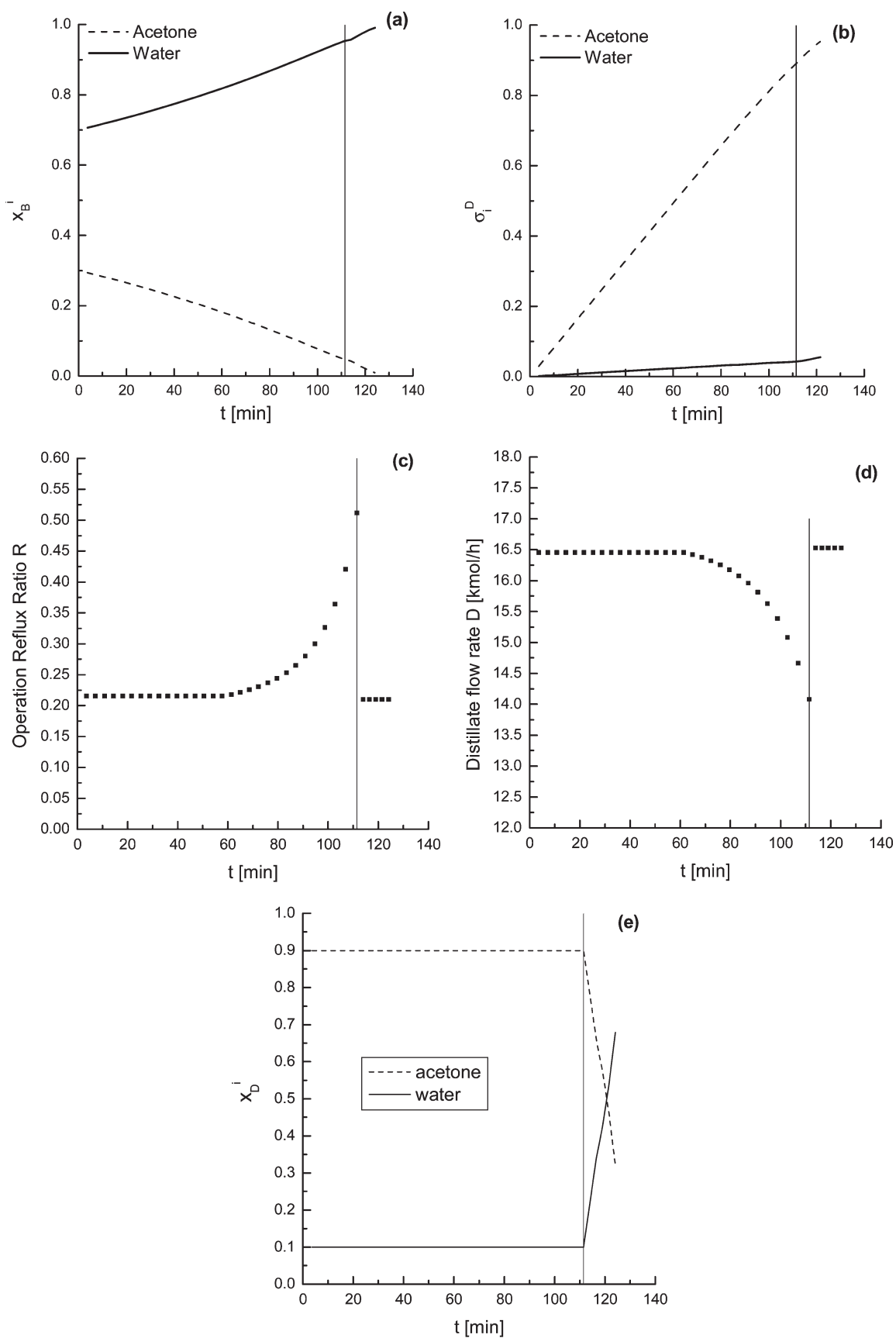


Figure 25. Time evolution of (a) still compositions, (b) fractional recoveries, (c) reflux ratio, (d) distillate flow rate, and (e) distillate compositions. $x_{i0}^B = 0.3$ (Region I).

Table 6. Results Corresponding to an Actual Design for $t_p = 2.07$ h

variable values at the end of each cut	main cut/specification	intermediate cut/specification
η (rectification advance)	0.297	0.3318
σ_A^R (acetone frac recovery)	$0.891 / \geq 0.89$	$0.99 / \geq 0.80$
$\langle x_A^D \rangle$ (mean distillate composition)	$0.9 / \geq 0.9$	0.7608
M [kmol] (molar holdup)	70.3	66.82
x_A^B (still mole fraction)	0.0465	$0.0093 / \leq 0.01$
operating and design variables		
R (operation reflux ratio)	variable, $1.05r$	constant, $1.05r$
N (number of stages)	6	3

rate V is obtained from the following equation:

$$V = \frac{1}{t_p} \int_0^{t_p} D(t)[R(t) + 1] dt$$

$$= \frac{1}{t_p} \int_0^\eta M_0[R(\eta) + 1] d\eta \quad (13)$$

Equation 13 can be integrated taking into account that $D_k(t) dt$ is the product amount recovered during the time interval $[t_{k-1}, t_k]$; i.e., $D_k(t) dt = M_0(\eta_k - \eta_{k-1}) = M_0 d\eta$.

An estimation of the minimum number of stages that are necessary to perform the separation can be obtained by solving a sequence of equilibria and mass balance computations (total reflux limiting condition) for a given initial still composition and cut specifications by assuming a differential rate of product withdrawal from the column at any time.¹² The actual number of stages can be approximated by either $N = 2N_{\min}$ or the typical construction¹¹ between the operating line and the equilibrium curve. Therefore, column size, utility loads, condenser, and reboiler sizes can be estimated for a specific design. Moreover, a quasi-optimal design can be achieved by simple enumeration of alternatives corresponding to different values of the operating time per batch t_p . Details of the design algorithm can be found in the contribution of Bernot et al.¹¹ Results from the optimization at the conceptual model level can then be used as initialization of a rigorous dynamic optimization of a batch rectifier with a finite number of equilibrium stages.¹³

Note that in this contribution, the accuracy of the conceptual model is assessed by comparing the instantaneous rectifier performance for a given still composition with the results given by steady-state simulations of a column section having 100 stages in Hysys.⁷ In this way, it was possible to approximate by simulation the behavior of profiles in a column with an infinite number of trays. The influence of both tray holdup and a finite number of stages must be taken into account at the rigorous optimization level, and for this reason, there is no sense in comparing here the performance of the model proposed in terms of a dynamic simulation. However, the results from the conceptual model enhances the performance of the dynamic optimization to find a near optimal design.¹³

Figure 25 shows the time evolution of the operation variables corresponding to an initial still composition $x_{i0}^B = 0.3$ (Figure 23). Simulation results correspond to an operating time per batch of 2.07 h and a molar amount of fresh feed per batch of 100 kmol. Hence, a vapor flow rate of 20 kmol/h is calculated from eq 13. The operation reflux ratio R was set as $1.05r$. Table 6 shows the

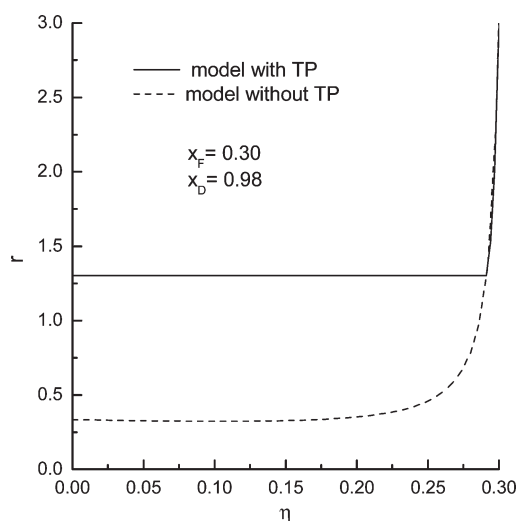


Figure 26. Performance comparison in terms of energy demand for the mixture acetone–water: models with and without considering the influence of tangent pinch points.

specifications of each cut in terms of product purities and fractional recoveries.

8. PERFORMANCE COMPARISON BETWEEN MODELS WITH AND WITHOUT TANGENT PINCH POINTS

Figure 26 shows the instantaneous minimum reflux ratio versus the rectification advance for a feed containing 30 mol % of acetone. While the upper solution was calculated from the model proposed here, the lower solution was estimated assuming that tangent pinch points do not control the separation; i.e., supposing that a node pinch with a composition identical to that of the instantaneous still composition determines the value of the instantaneous minimum reflux ratio. Both models were integrated until a value of $\eta = 30\%$ for the rectification advance. The acetone mole fraction in the product is 98 mol %. For the considered example, the minimum amount of vapor $\langle V \rangle_{\text{withTP}}$ [kmol] that must be generated to achieve the separation as calculated taking into account the influence of tangent pinch points is very different from the value $\langle V \rangle_{\text{withoutTP}}$ [kmol] predicted for the simplest model. In fact, $\langle V \rangle_{\text{withTP}} = 1.594 \langle V \rangle_{\text{withoutTP}}$.

9. CONCLUDING COMMENTS AND FUTURE WORK

On the basis of pinch theory, a conceptual model for the instantaneous rectifier performance is proposed in order to deal with the appearance of tangent pinch points in batch distillation of binary mixtures. Incorporated into a model for the whole column, both operation at constant reflux ratio and constant distillate composition are taken into account. Results obtained from this approach either at a design level or at an optimization level are suitable for rigorous optimization of the operation. They may be also used to throw light upon issues like novelty, academic relevance and practical interest of the conceptual model presented here.

In the motivating paper by Bernot et al.,¹¹ the authors stated that the treatment of nonideal mixtures would be straightforward and would require only an efficient method for computing pinch compositions. This paper, however, demonstrates that several algorithms are needed to capture the different operation modes

that can be found in the batch distillation of highly nonideal binary mixtures. Moreover, the incorporation of the model into a software of conceptual design¹² requires algorithms for azeotrope and inflection points calculations, topology analysis for the determination of distillation regions and perfect split analysis to determine maximum feasible cuts.

The relevance issue can be assessed from the analysis of results obtained by Brueggemann et al.¹³ There, a combination of a conceptual model for a distillation column based on pinch theory (the rectification body method^{14–16}), and dynamic optimization is proposed. It is intended to determine an optimal or at least a good suboptimal separation process design and operation in a more efficient way. Actually, they discuss how a fast conceptual design method based on the rectification body method for the design of continuously operated columns can be utilized to significantly improve performance and robustness of rigorous optimization-based design methods.

Other relevant areas in which the conceptual modeling approach is meaningful are operation control of batch distillations¹⁷ and synthesis and design of novel pressure swing batch distillations like the double column arrangement proposed by Modla and Lang.¹⁸

Finally, the present importance of distillation is documented by the fact that approximately 40 000 distillation columns are in operation in the USA alone. They consume about 7% of the total energy demand of the mentioned country.¹⁹ Models like the one presented in this paper can be used in the synthesis and design of processes for the recovery of spent solvents in pharmaceutical companies. In this case, hybrid technologies like distillation plus membrane separation are emerging alternatives which deserve further research work.

AUTHOR INFORMATION

Corresponding Author

*E-mail: destila@santafe-conicet.gov.ar.

ACKNOWLEDGMENT

The authors gratefully acknowledge the financial support of this work to CONICET, UNL, and ANPCyT.

NOMENCLATURE

D = distillate flow rate

$D_k(t)$ = product amount recovered in the time interval $[t_{k-1}, t_k]$

dy/dx = first derivative of vapor mole fraction with respect to liquid mole fraction

d^2y/dx^2 = second derivative of vapor mole fraction with respect to liquid mole fraction

F = total amount of fresh feed

$f(x)$ = nonlinear equation

IMM = improved memory method

L = liquid phase (in figure axis titles)

L_N = flow rate of the stream feeding the boiler

M_0, M = molar amount of fresh feed per batch, molar holdup in the still

m_{x_B, x_D} = slope of the segment joining x_B and x_D

m_{x_p} = slope of the tangent to the equilibrium curve at x_p

N = number of stages

N_{\min} = minimum number of stages

n_b = number of batches

p_i^0 = vapor pressure of component i

r, R = reflux ratio, operation reflux ratio defined as $1.05r$

r_{bif} = bifurcation reflux ratio

r_{max} = maximum reflux ratio for which the minimum energy demand of the column is controlled by a tangent pinch

r_{max}^0 = maximum reflux ratio for which the minimum energy demand of the column is controlled by a node pinch

r^* = limiting reflux ratio

T = temperature

t = time

t_d = dead time

t_p = operation time per batch

t_w = time available

$\langle V \rangle$, V = minimum vapor amount with (withTP) or without (withoutTP) tangent pinch, vapor flow rate

x^* = root of the nonlinear equation $f(x)$

$x_B, y_{x_B}^*$ = still composition, vapor in equilibrium with x_B

$x_B^{\text{lim}}, y_{x_B}^{*, \text{lim}}$ = limiting liquid composition between Region 0 and Region I, vapor in equilibrium with x_B^{lim}

x_i^D = instantaneous distillate composition

$x_{\text{IP}}, y_{x_{\text{IP}}}^*$ = inflection point composition, vapor in equilibrium with x_{IP}

$x_p, y_{x_p}^*$ = controlling pinch composition, vapor in equilibrium with x_p

$x_{i0}^B, x_{A,0}^B, x_A^B$ = initial mole fraction of component i in the still, initial mole fraction of acetone in the still, instantaneous mole fraction of acetone

x_p^{node} = node pinch composition

x_p^{saddle} = saddle pinch composition

x_D = distillate composition

$x_{D, \text{calc}}$ = distillate composition calculated in section 5.1

x_N = liquid composition of the stream feeding the boiler

V = vapor phase (in figure axis titles)

$z_{D, \text{crit}}$ = critical distillate composition

Variables Involving Greek Letters

Δm = error function defined in terms of slopes

Δr = error function defined in terms of reflux ratios

Δx_D = error function defined in terms of distillate compositions

Ψ = approximation of the inverse function of $f(x)$

$\langle \varepsilon_D^{\text{rel}} \rangle$ = mean relative error in distillate composition

$\varepsilon_D^{\text{rel, max}}$ = maximum relative error in distillate composition

γ_i = activity coefficient of component i

η = rectification advance

σ_i^D, σ_A^D = fractional recovery of the component i in the distillate, fractional recovery of acetone in the distillate

REFERENCES

- (1) Doherty, M. F.; Malone, M. F. *Conceptual Design of Distillation Systems*, 2001, *McGraw-Hill Higher Education*; New York.
- (2) Fidkowski, Z. T.; Malone, M. F.; Doherty, M. F. Nonideal Multicomponent Distillation: Use of Bifurcation Theory for Design. *AIChE J.* **1991**, *37* (12), 1761–1779.
- (3) Lucia, A.; Amale, A.; Taylor, R. Distillation pinch points and more. *Comput. Chem. Eng.* **2008**, *32*, 1342–1364.
- (4) Torres, K. A.; Espinosa, J. Incorporating Tangent Pinch Points into the Conceptual Modelling of Batch Distillations: Ternary Mixtures. *Ind. Eng. Chem. Res.* **2009**, *48* (2), 857–869.
- (5) Salomone, H. E.; Chiotti, O. J.; Iribarren, O. A. Short-Cut Design Procedure for Batch Distillations. *Ind. Eng. Chem. Res.* **1997**, *36* (1), 130–136.
- (6) Espinosa, J.; Salomone, E.; Iribarren, O. Computer-Aided Conceptual Design of Batch Distillation Systems. *Ind. Eng. Chem. Res.* **2004**, *43*, 1723–1733.

- (7) *Hysys User Manual*; Hyprotech Ltd.: Calgary, Canada, 1999.
- (8) Shacham, M. An Improved Memory Method for the Solution of a Nonlinear Equation. *Chem. Eng. Sci.* **1989**, *44* (7), 1495–1501.
- (9) Taylor, R.; Kooijman, H. A. Composition Derivatives of Activity Coefficient Models. *Chem. Eng. Commun.* **1991**, *102*, 87–106.
- (10) Poellmann, P.; Blass, E. Best Products of Homogeneous Azeotropic Distillations. *GAS Sep. Purif.* **1994**, *8* (4), 194–228.
- (11) Bernot, C.; Doherty, M. F.; Malone, M. F. Design and Operating Targets for Nonideal Multicomponent Batch Distillation. *Ind. Eng. Chem. Res.* **1993**, *32*, 293–301.
- (12) Espinosa, J.; Salomone, E. *Conceptual Batch Distillation Toolkit 3.0 User Manual*; Santa Fe, Argentina, 2001.
- (13) Brueggemann, S.; Oldenburg, J.; Marquardt, W. Combining Conceptual and Detailed Methods for Batch Distillation Process Design. *Proceedings of FOCAPD*; Floudas, C. A.; Agrawal, R., Eds.; Elsevier: New York, 2004; pp 247–250. July 11–16, 2004. Princeton, New Jersey.
- (14) Bausa, J.; v. Watzdorf, R.; Marquardt, W. Shortcut Methods for Nonideal Multicomponent Distillation: 1. Simple Columns. *AIChE J.* **1998**, *44* (10), 2181–2198.
- (15) Bausa, J. *Näherungsverfahren für den konzeptionellen Entwurf und die thermodynamische Analyse von destillativen Trennprozessen*; Fortschritt-Berichte VDI: Düsseldorf, 2001; Reihe 3, p 692.
- (16) Espinosa, J.; Brueggemann, S.; Marquardt, W. Application of the Rectification Body Method to Batch Rectification. *European Symposium on Computer Aided Process Engineering-15*, 20A; Puigjaner, L., Espuña, A., Eds.; Elsevier: New York, 2005; pp 757–762. May, 29–June, 1. Barcelona, Spain.
- (17) Espinosa, J.; Marchetti, J. L. Conceptual Modeling and Referential Control Applied To Batch Distillations. *Ind. Eng. Chem. Res.* **2007**, *46*, 6000–6009.
- (18) Modla, G.; Lang, P. Feasibility of New Pressure Swing Batch Distillation Methods. *Chem. Eng. Sci.* **2008**, *63*, 2856–2874.
- (19) Stichlmair, J.; Fair, J. *Distillation: Principles and Practice*; Wiley-VCH: New York, 1998.